Tilted axis rotations in ^{182}Os

Yukio Hashimoto
with
Takatoshi Horibata
Department of Software and Information Technology,
Aomori University, Aomori, Aomori 030-0943, Japan

Contents

1. Introduction:

general modes of nuclear rotation

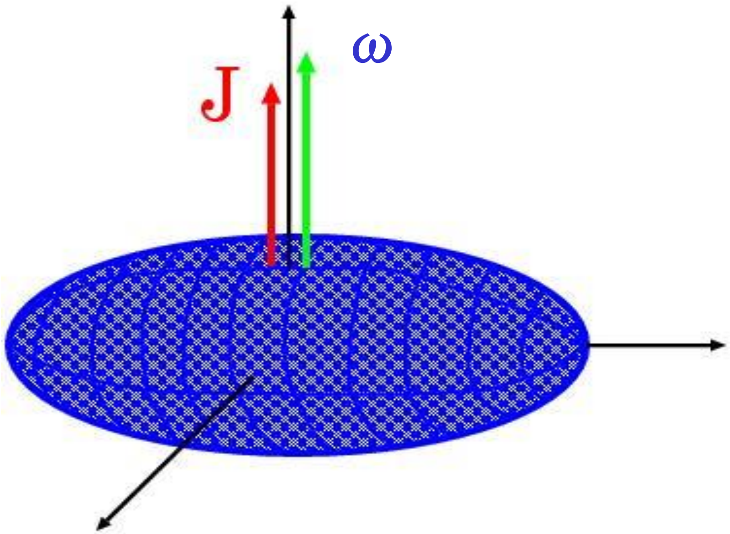

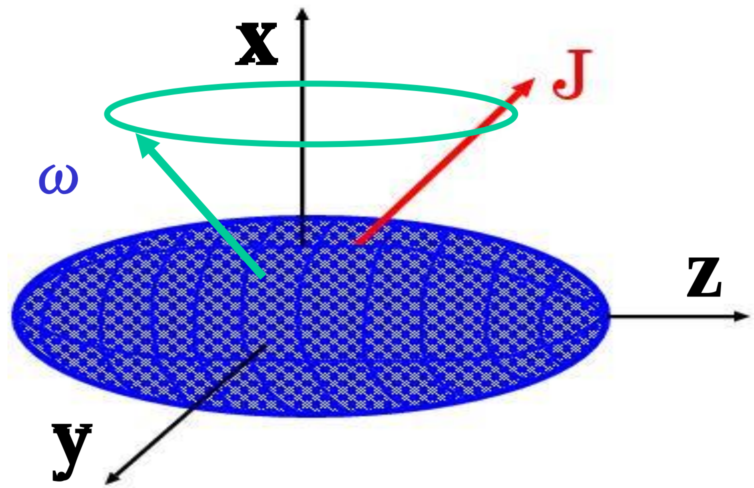

wobbling motion

tilted axis rotation

(high K t-band)

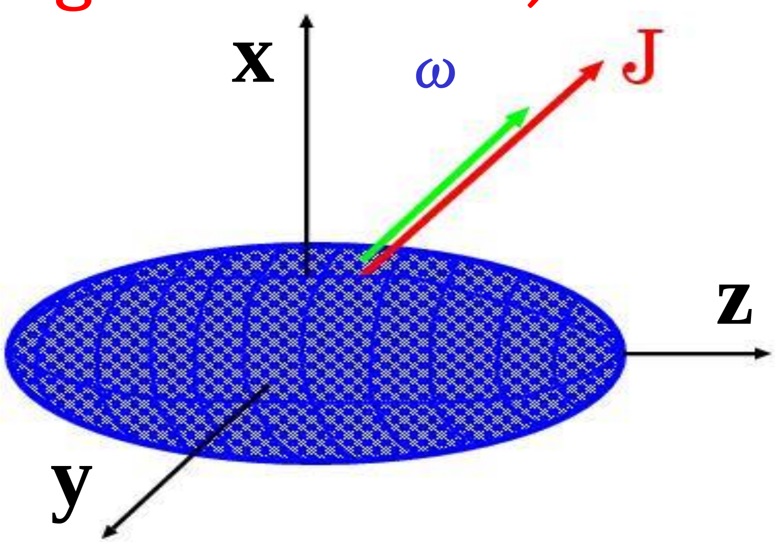

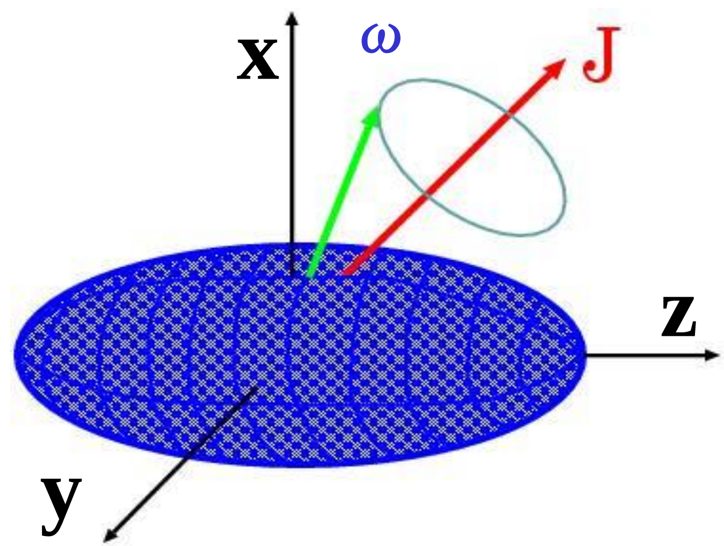

wobbling band

Odegard et al.
Phys.Rev.Lett.86(2001), 5866

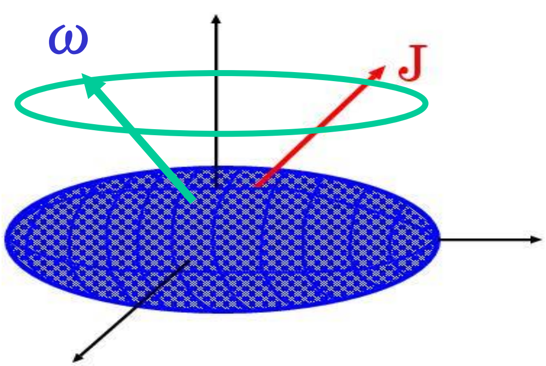

triaxial, strongly deformed (TSD) bands has been given, but one possible and unique consequence of a rotating nucleus with a triaxial shape is the existence of "wobbling bands" [2].

In an investigation of the isotopes ^{163,164}Lu with the Euroball III array [11], a second band (TSD2) with similar properties as the previously known $i_{13/2}$ band (TSD1) has been observed in ^{163}Lu [12]. This second band was found to decay to TSD1, but no connections could be established. The new band was considered [12] a candidate for a wobbling excitation. The present work firmly establishes the band as a wobbling excitation built on TSD1.

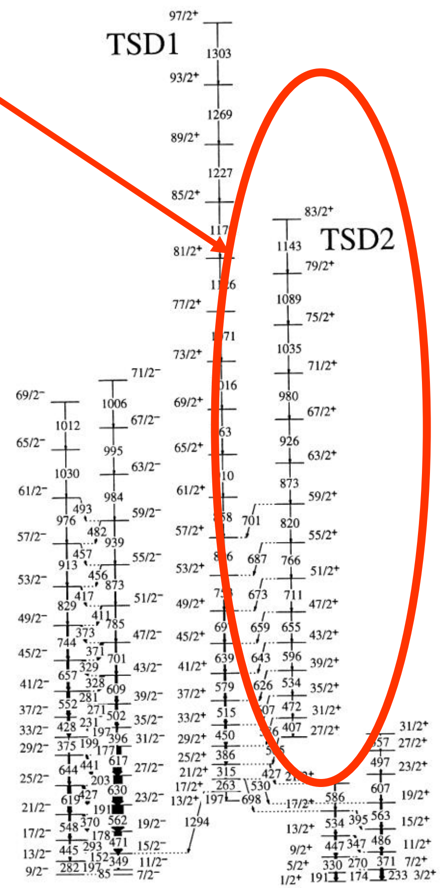

FIG. 1. Partial level scheme of ^{163}Lu showing the two TSD bands together with the connecting transitions and the ND structures to which the TSD states decay.

To find and investigate the nature of the connecting transitions between TSD2 and TSD1, an experiment was performed with Euroball IV [11] in Strasbourg equipped with the BGO inner ball. With the ^{139}La(^{29}Si, $5n$)^{163}Lu reaction and a beam energy of 152 MeV, approximately 2.4×10^9 events with 3 or more Compton suppressed γ rays in the Ge detectors and 8 or more γ rays detected in the BGO inner ball were collected and used in 3D and 4D coincidence analyses.

The band TSD2 could be extended to both lower ($6\hbar$) and higher ($4\hbar$) spins, and 9 connecting transitions to TSD1 were established; see Fig. 1. Furthermore, TSD1 has been extended $10\hbar$ higher in spin. Gated spectra illustrating the connecting transitions and their angular dependence, as well as in-band transitions in TSD1 and TSD2 in the same energy range, are shown in Fig. 2. The population of TSD1 and TSD2 relative to yrast are ~10% and ~2.5%, respectively.

A determination of the multipolarity of the connecting transitions is crucial. The directional correlation of γ rays from the oriented states (DCO ratios) [13] were obtained for the strongest connecting transitions using "25°" and "90°" data. In addition, angular distribution ratios were produced from the same data. Linear polarization measurements were also attempted using the two "90°" rings of Clover detectors [11]. In all cases the data were selected by clean gates in TSD1 in any angle in the spin range $21/2 - 45/2\hbar$. The spin alignment, parametrized as σ/I for a Gaussian distribution of the m-substate population, $P_m(I) \propto \exp(-\frac{m^2}{2\sigma(I)^2})$ [14], was determined for a number of stretched electric quadrupole ($E2$) transitions in the same spin region as the connecting transitions. There was no detectable spin dependence. An average value is $\sigma/I = 0.25 \pm 0.02$. Both the angular correlation and angular distribution data are consistent with mixed $M1/E2$ multipolarity for the connecting transitions. Within

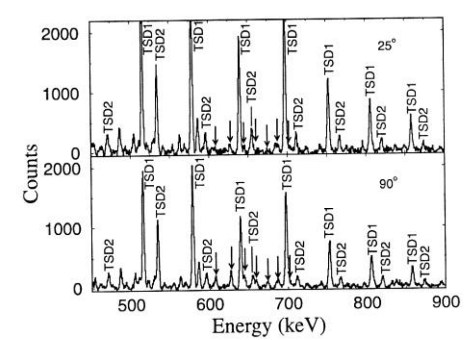

FIG. 2. Spectra from the angular distribution matrices gated on the 450 keV transition in TSD1. Connecting transitions are marked by arrows. Most other unmarked transitions belong to the decay of TSD1.

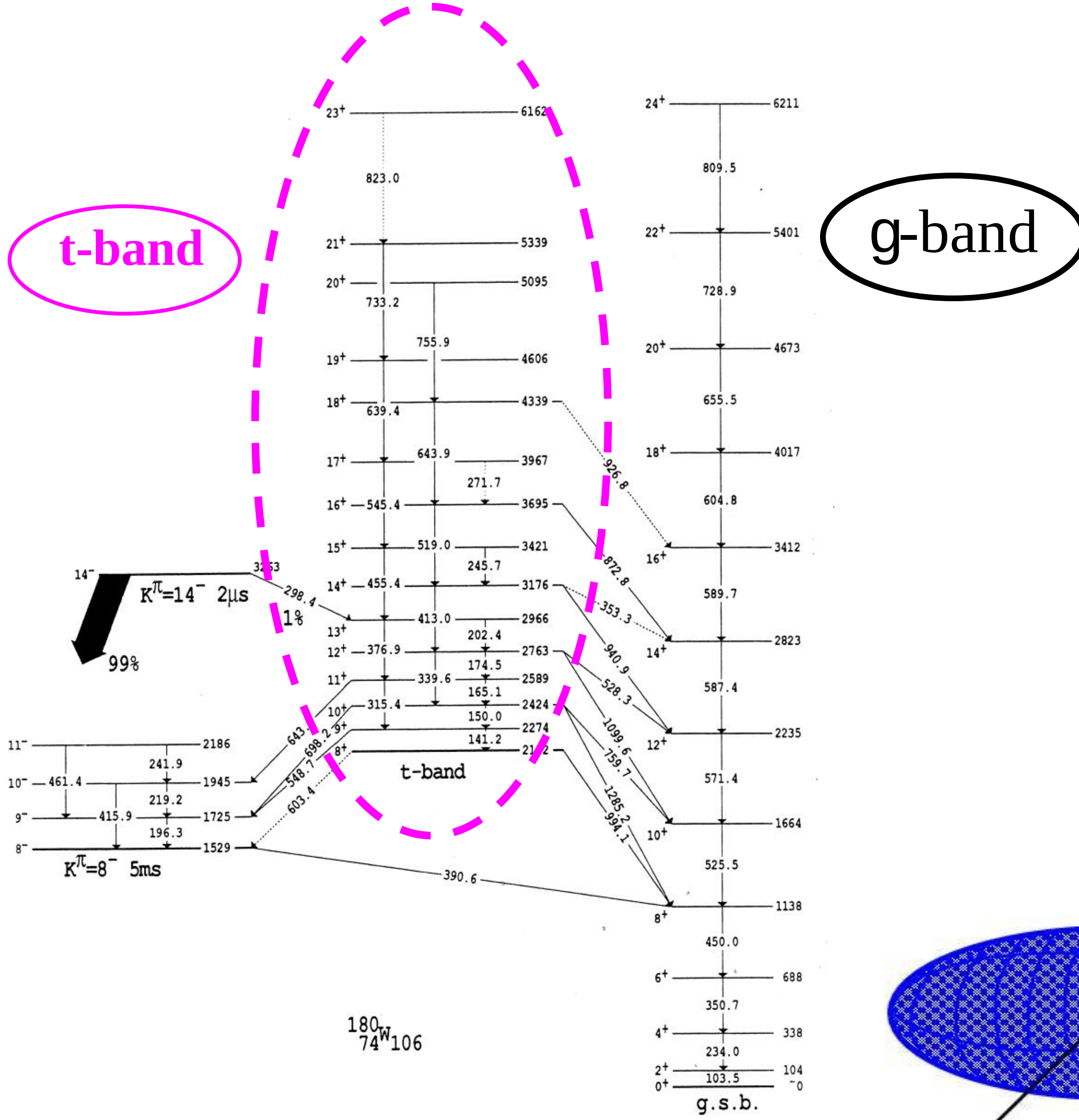

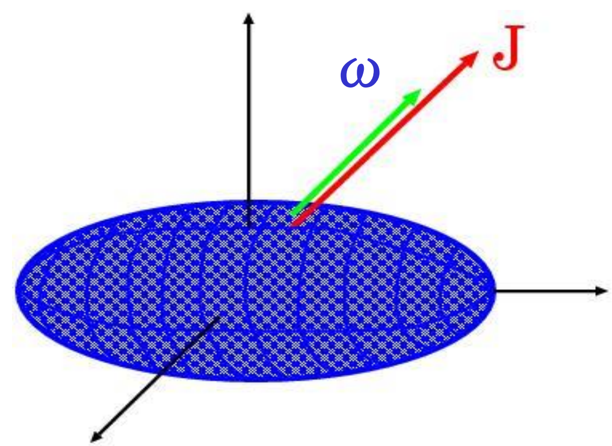

P.M.Walker et al., Phys. Lett. B309(1993), 17-22.

^{182}Os

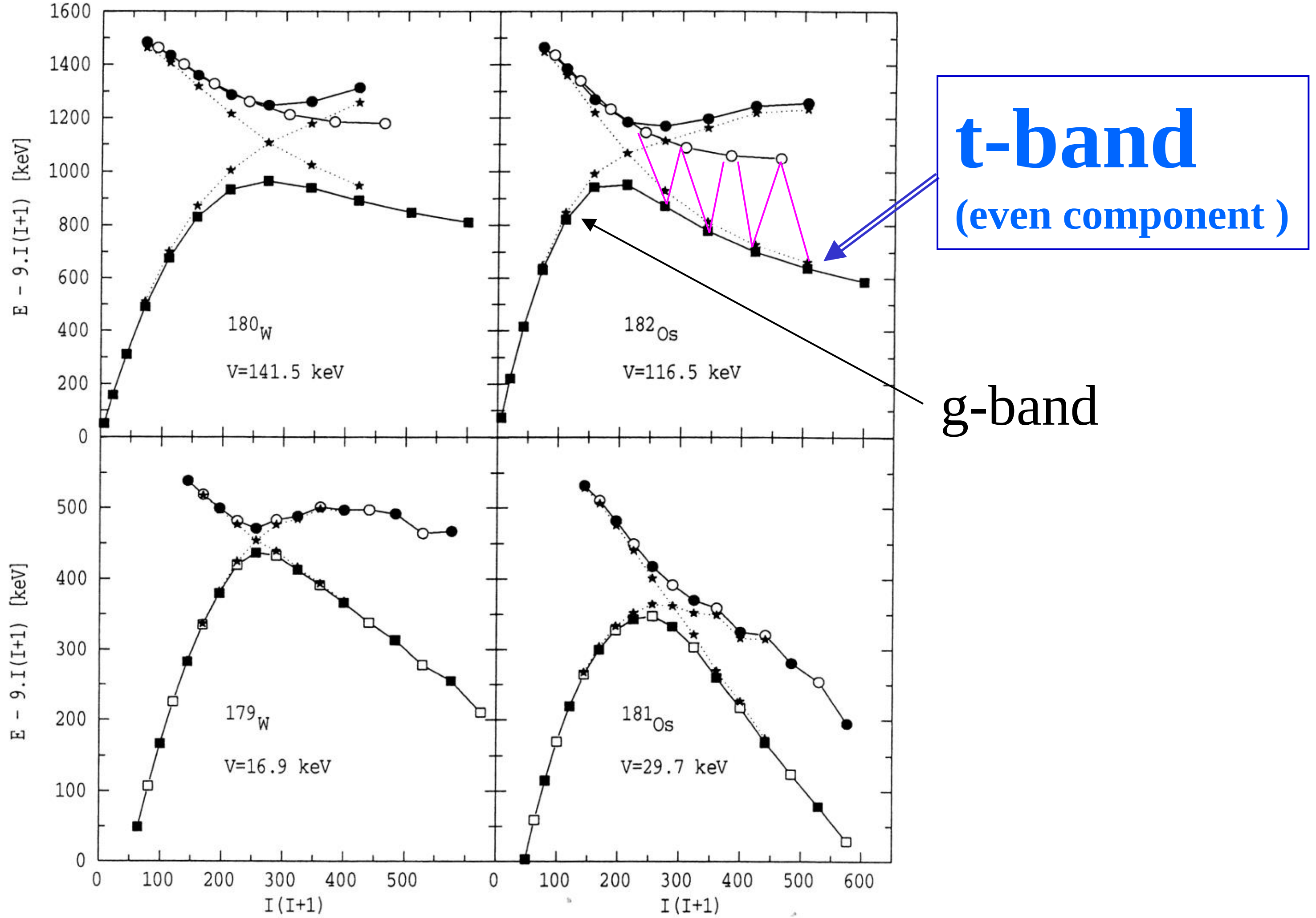

P.M.Walker et al., Phys. Lett. B309(1993), 17-22.

theoretical frameworks

Rigid rotor

A. Bohr and B. R. Mottelson, *Nuclear Sructure*, Vol. II, p.190 (1975).

TAC

*S. Frauendorf, Nucl. Phys. A557, 259c(1993)
*S. Frauendorf, Nucl. Phys. A677, 115(2000).
*S. Frauendorf, Rev. Mod. Phys. 73, 463(2001).

HFB+RPA

*M. Matsuzaki, Nucl. Phys. A509, 269(1990).
*Y. R. Shimizu and M. Matsuzaki, Nucl. Phys. A588, 559(1996).
*M. Matsuzaki, Y. R. Shimizu and K. Matsuyanagi, Phys. Rev. C65, 041303(R)(2002).
*M. Matsuzaki, Y. R. Shimizu and K. Matsuyanagi, Phys. Rev. C69, 034325(2004)

HFB+GCM

*A. K. Kerman and N. Onishi, Nucl. Phys. A361, 179(1981).
*N. Onishi, Nucl. Phys. A456, 279(1986).
*T. Horibata and N. Onishi, Nucl. Phys. A596, 251(1996).
*T. Horibata, M. Oi, N. Onishi and A. Ansari, Nucl. Phys. A646, 277(1999); A651, 435(1999).
*Y. Hashimoto and T. Horibata, Phys. Rev. C74, 017301(2006)
*Y. Hashimoto and T. Horibata, EPJ A42, 571(2009).

2. Three-dimensional cranked HFB

A.K.Kerman and N.Onishi, Nucl.Phys.A361(1981),179

$$\frac{d\mathbf{j}}{dt} = \mathbf{j} \times \vec{\omega}$$

$$\vec{\omega} - (\mathbf{R} \times (\mathbf{j} \times \vec{\omega})) = \vec{\mu}$$

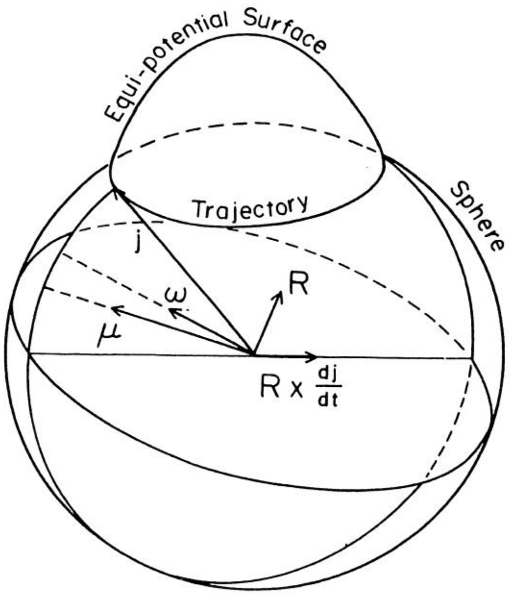

$$\vec{\mu} = \frac{\partial \mathcal{H}(\mathbf{j})}{\partial \mathbf{j}}$$

$$\mathbf{R} = \nabla \times \mathbf{S} \qquad \mathbf{S} = \langle \Phi(\mathbf{j}) | i \frac{\partial}{\partial \mathbf{j}} | \Phi(\mathbf{j}) \rangle$$

$$\delta \langle \Phi(\mathbf{j}) | \hat{H} - \vec{\mu} \cdot \hat{\mathbf{J}} - \vec{\xi} \cdot \hat{\mathbf{B}} | \Phi(\mathbf{j}) \rangle = 0$$

$$\hat{\mathbf{B}} = (yz, zx, xy)$$

Constraints used in HFB calculation

$$\langle J_x \rangle = J_0 \cos \psi \quad \langle J_z \rangle = J_0 \sin \psi$$

$$\langle J_y \rangle = 0$$

$$\langle yz \rangle = 0 \quad \langle zx \rangle = 0 \quad \langle xy \rangle = 0$$

$$\langle \hat{N}_p \rangle = Z \quad \langle \hat{N}_n \rangle = N$$

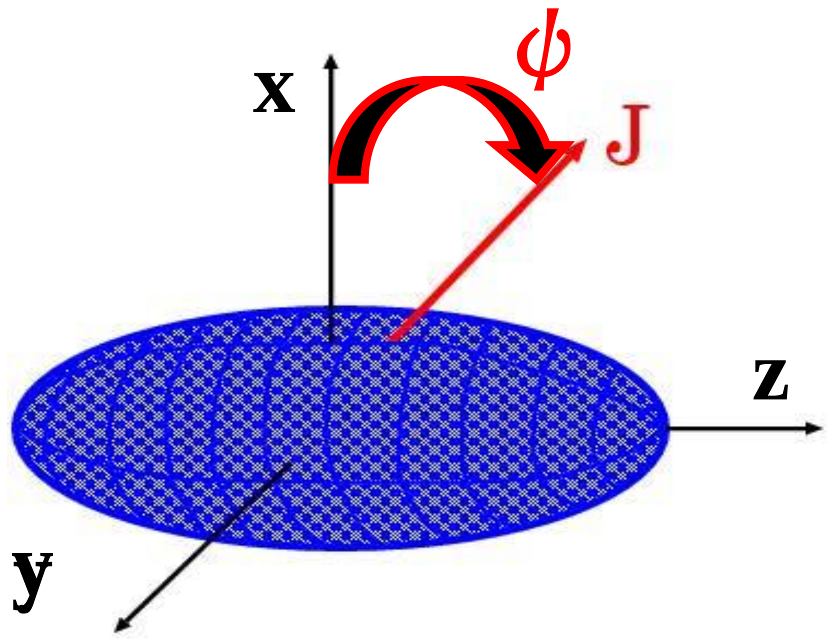

Starting points of tilted wave functions

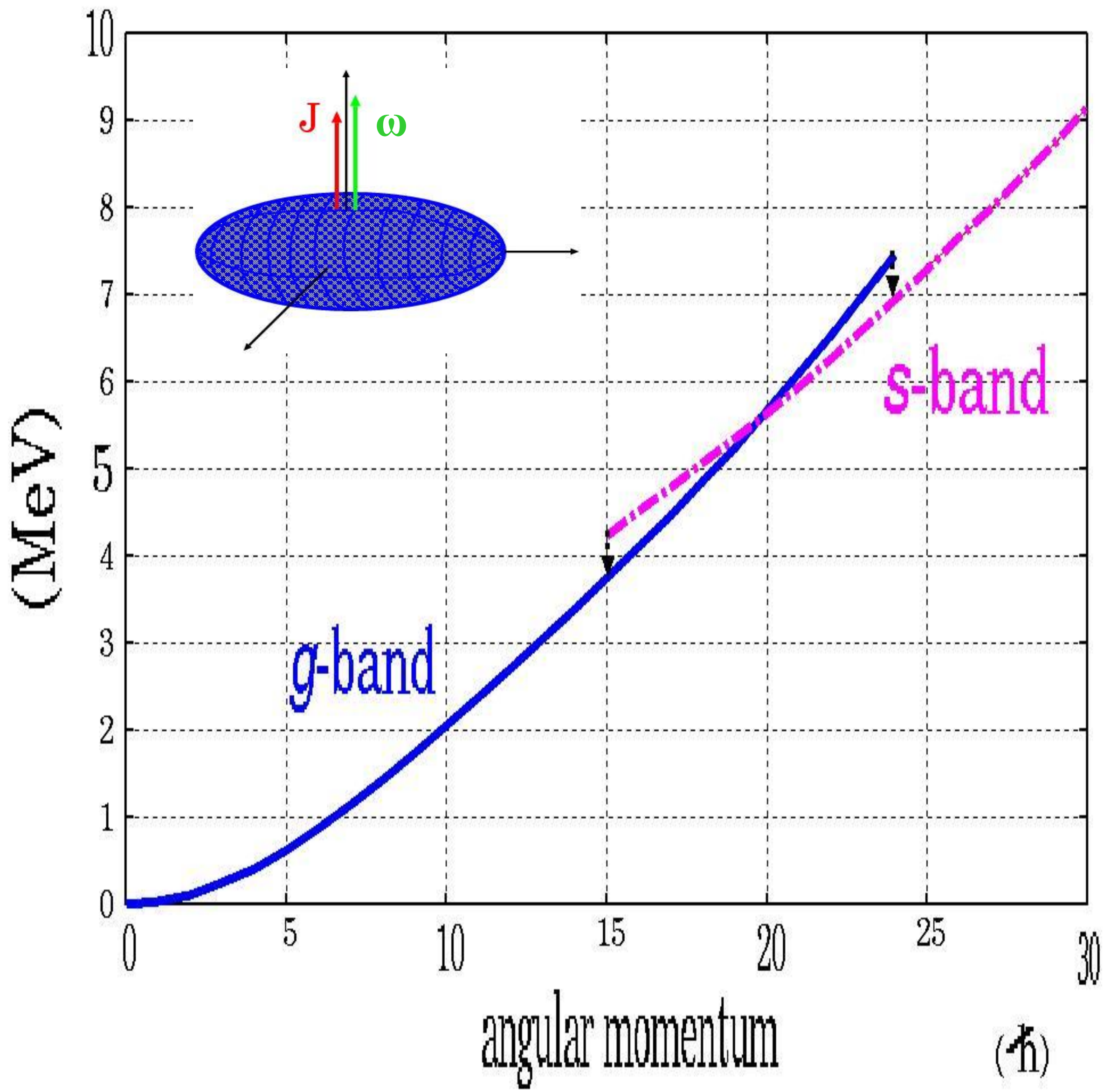

Energy vs tilt angle

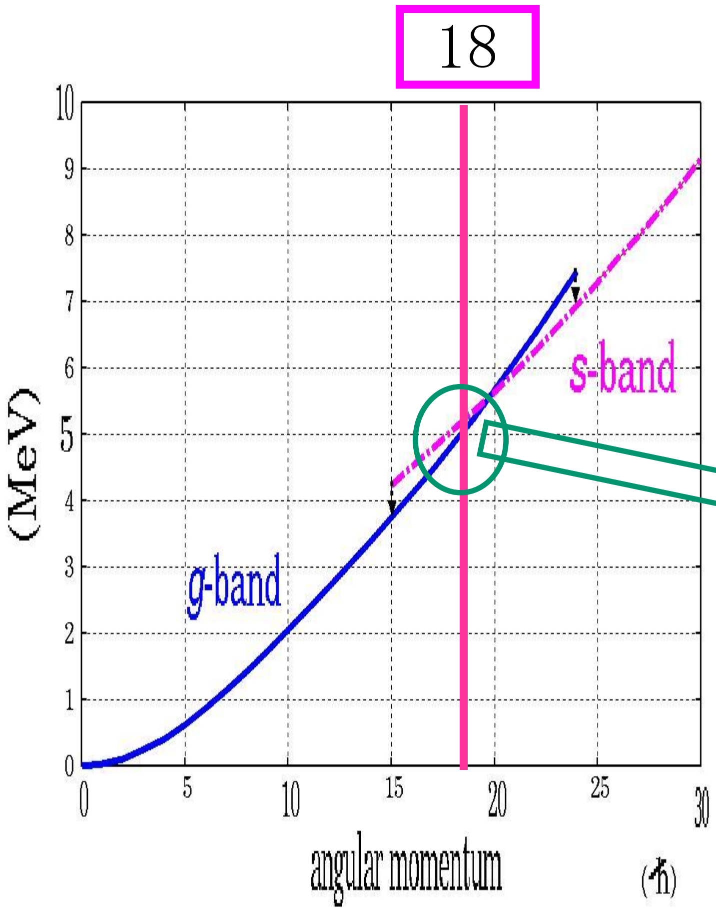

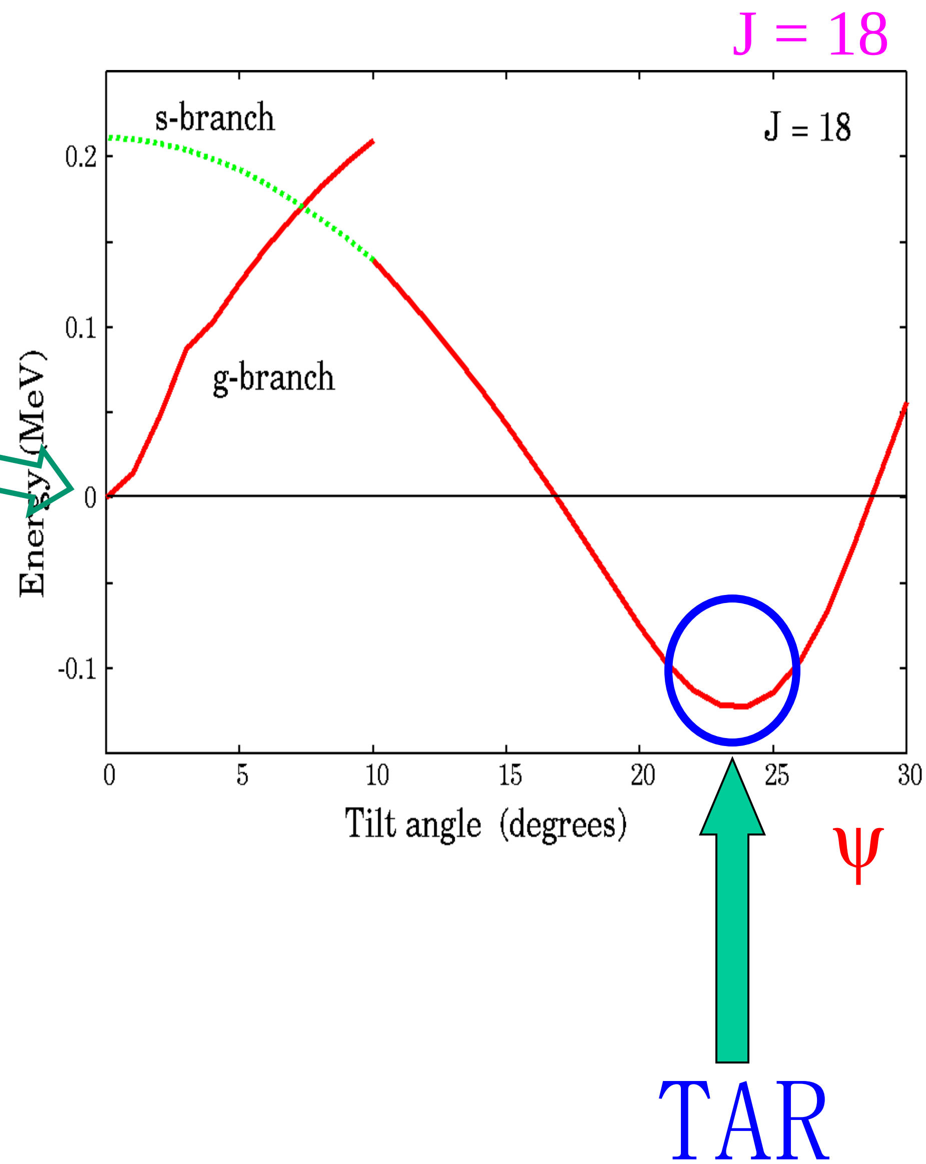

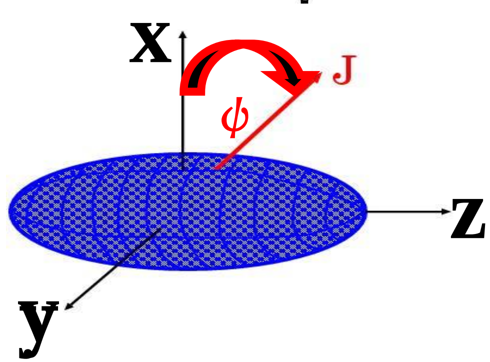

TAR states and K=8 band

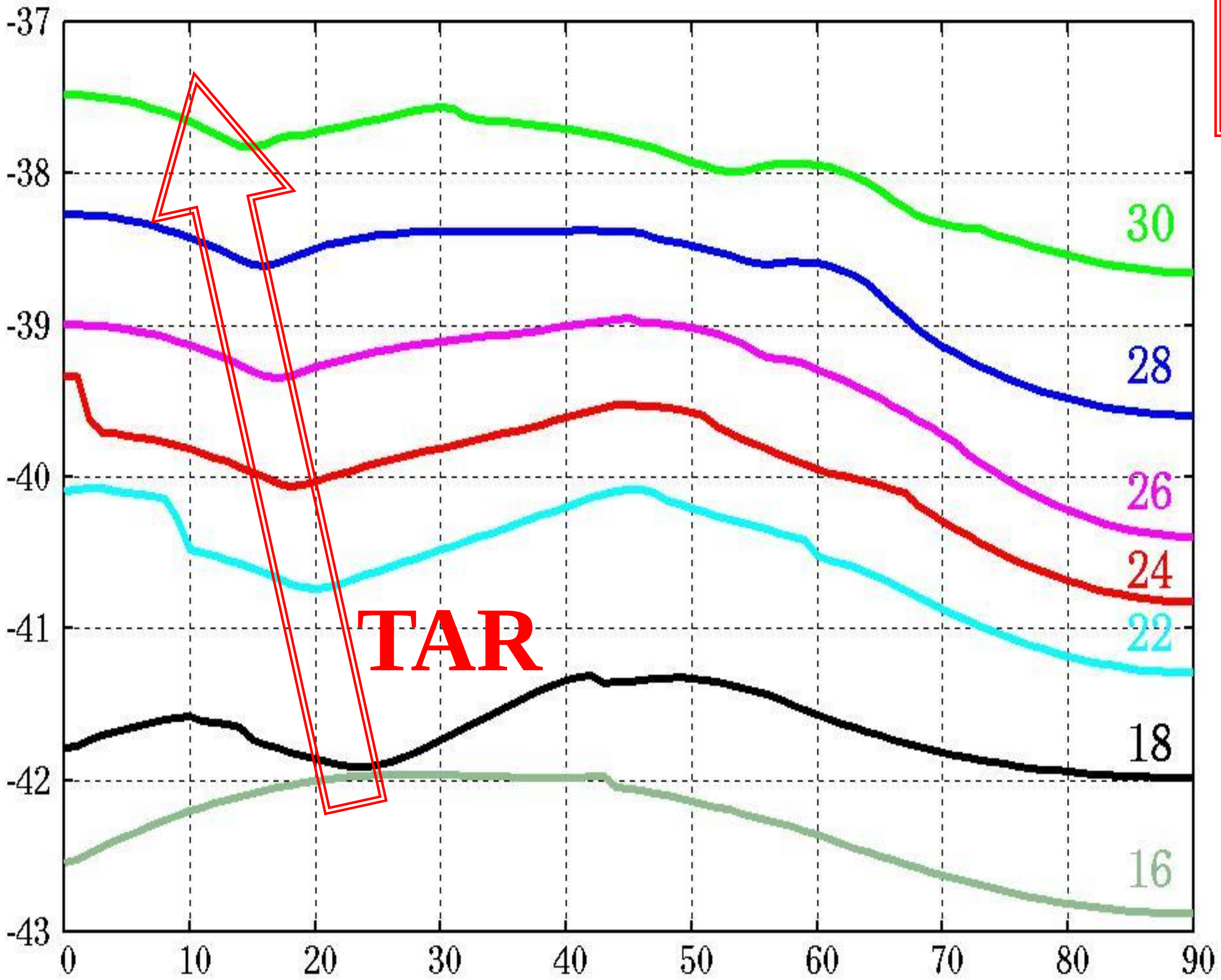

tilt angle (degree)

K ～ const.

30 * sin(15°) = 7.8

28 * sin(16°) = 7.7

26 * sin(17°) = 7.6

24 * sin(18°) = 7.6

22 * sin(20°) = 7.5

18 * sin(24°) = 7.3

TAR states (K=8 band)

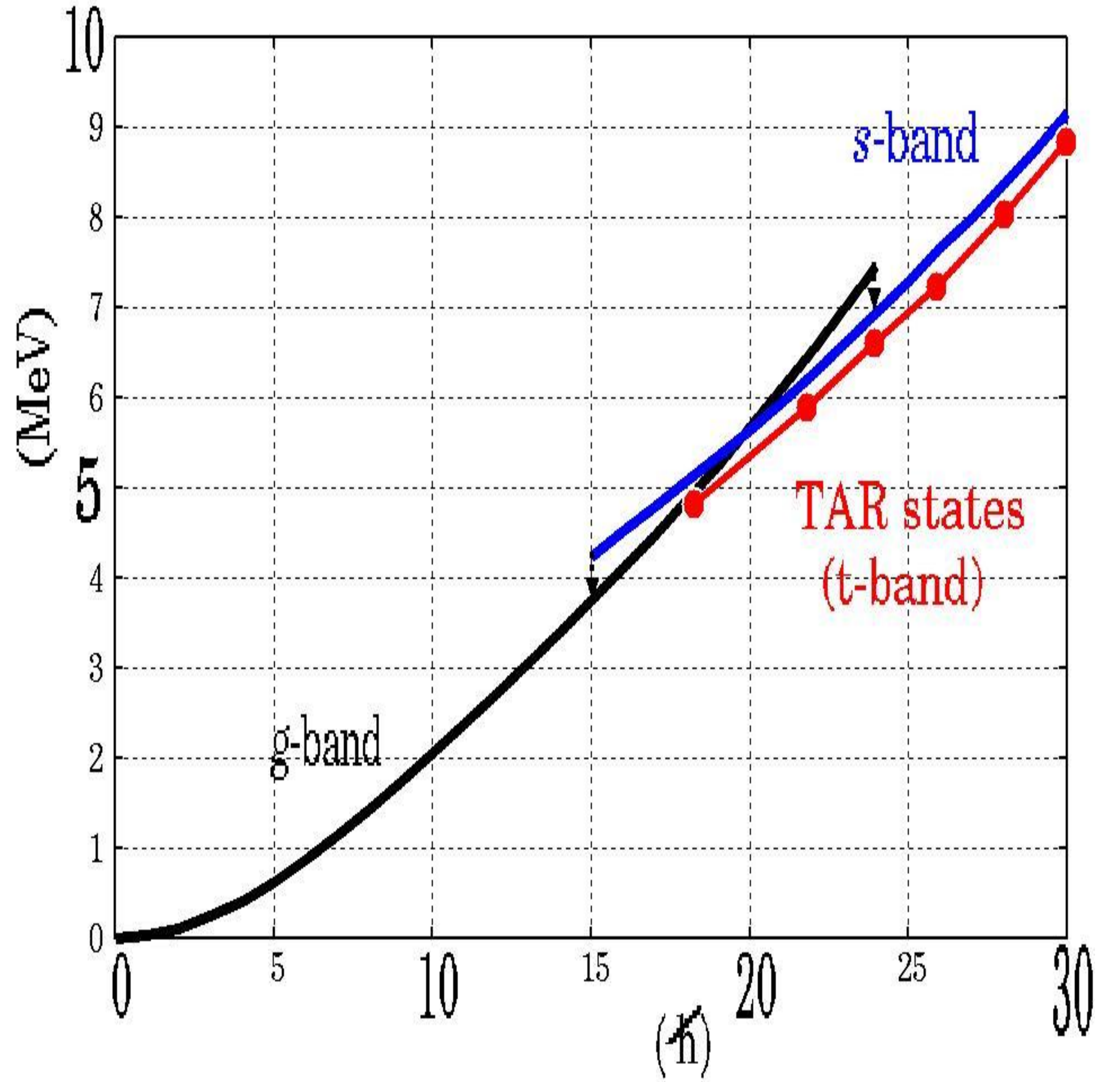

angular momentum J

3. Tilted states and GCM

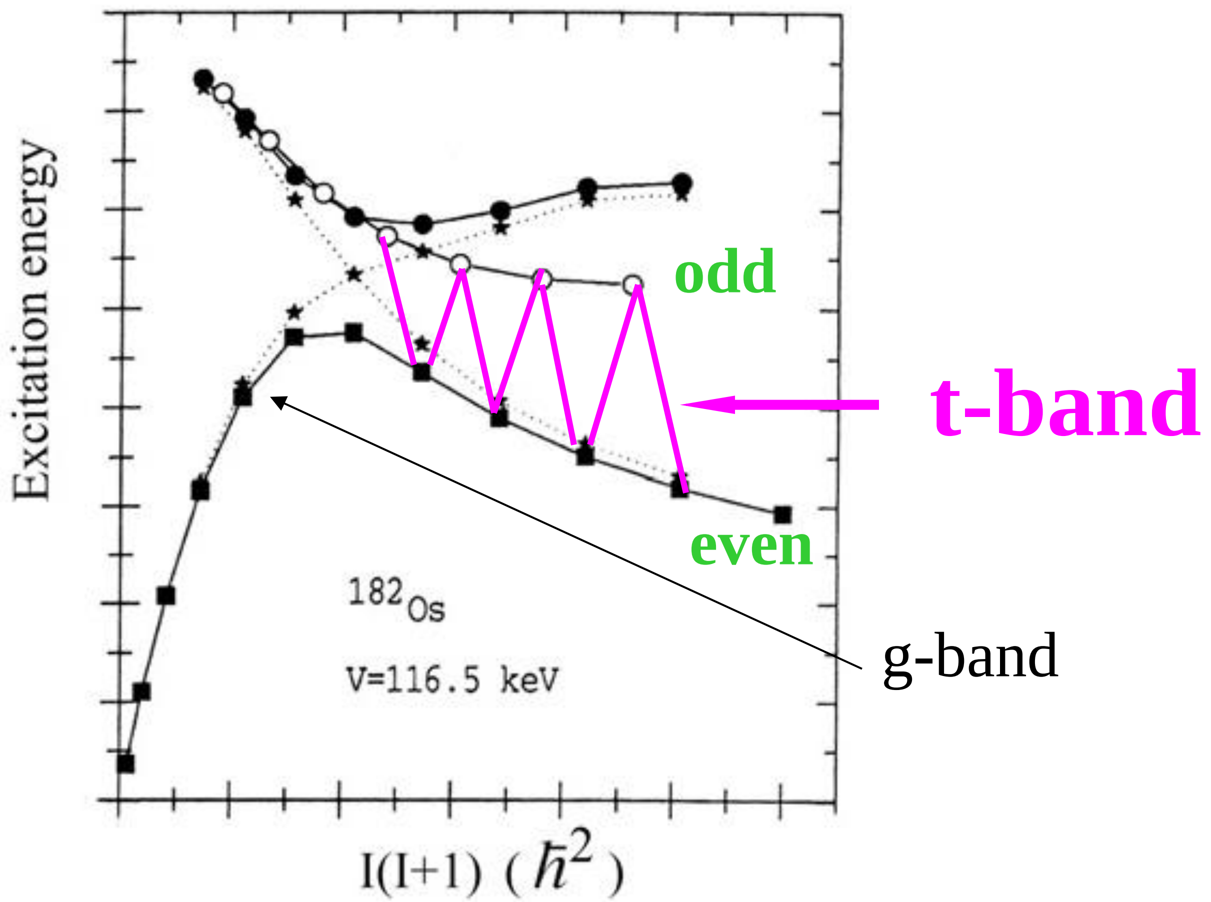

P.M.Walker et al., Phys. Lett. B309, 17-22(1993).

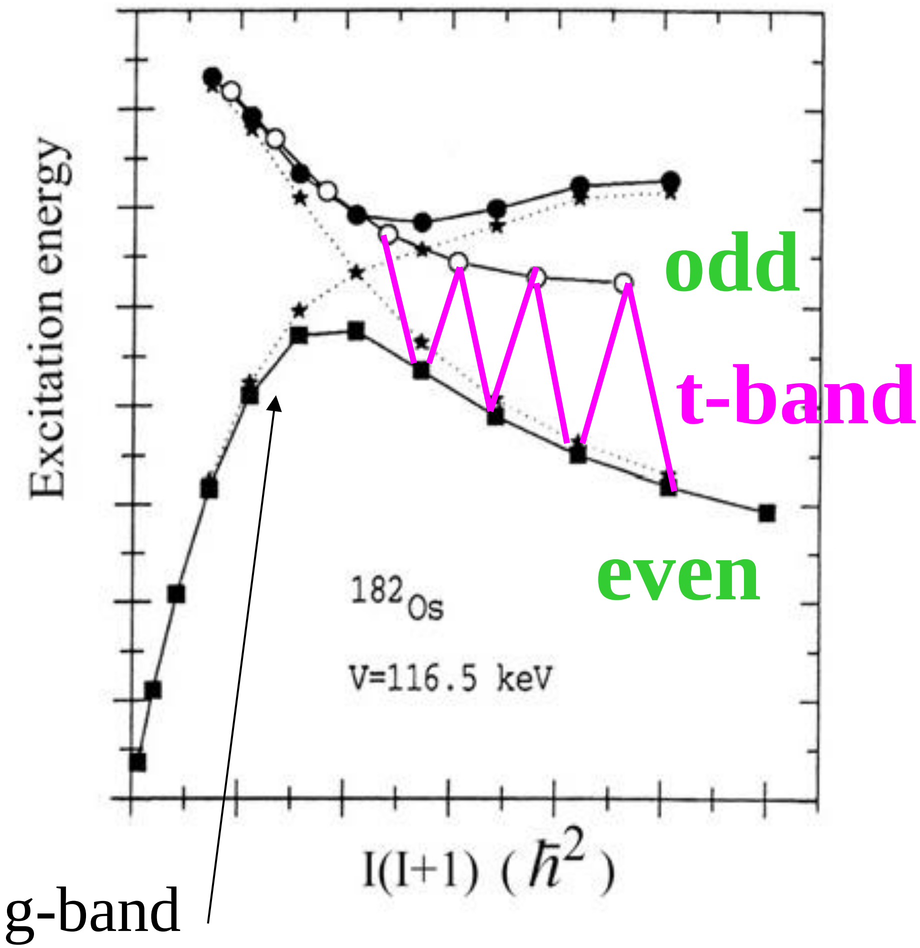

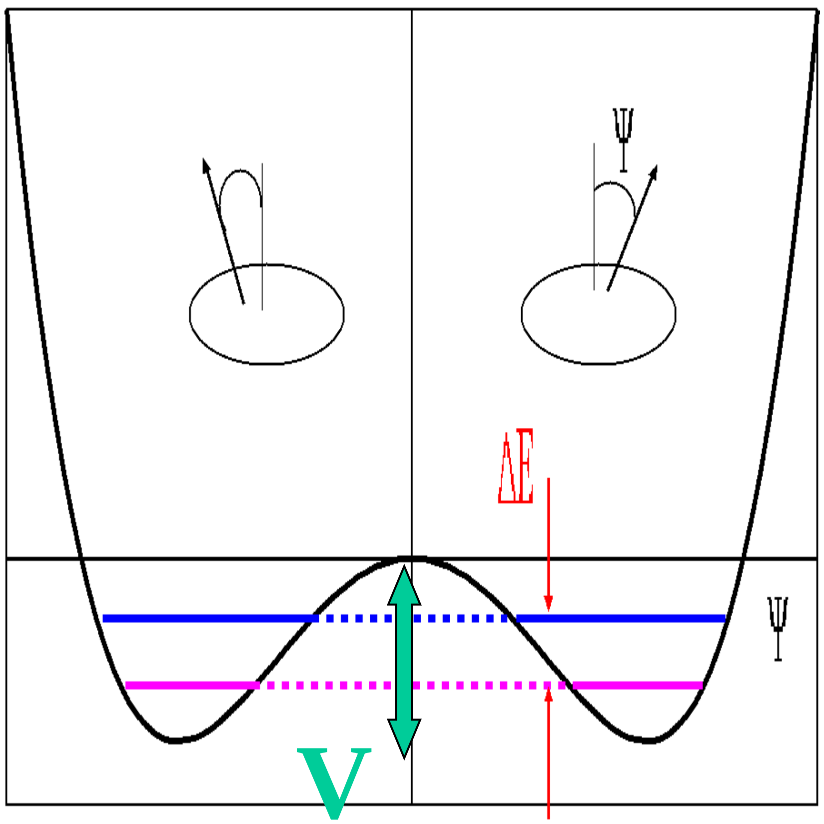

P.M.Walker et al., Phys. Lett. B309(1993), 17-22.

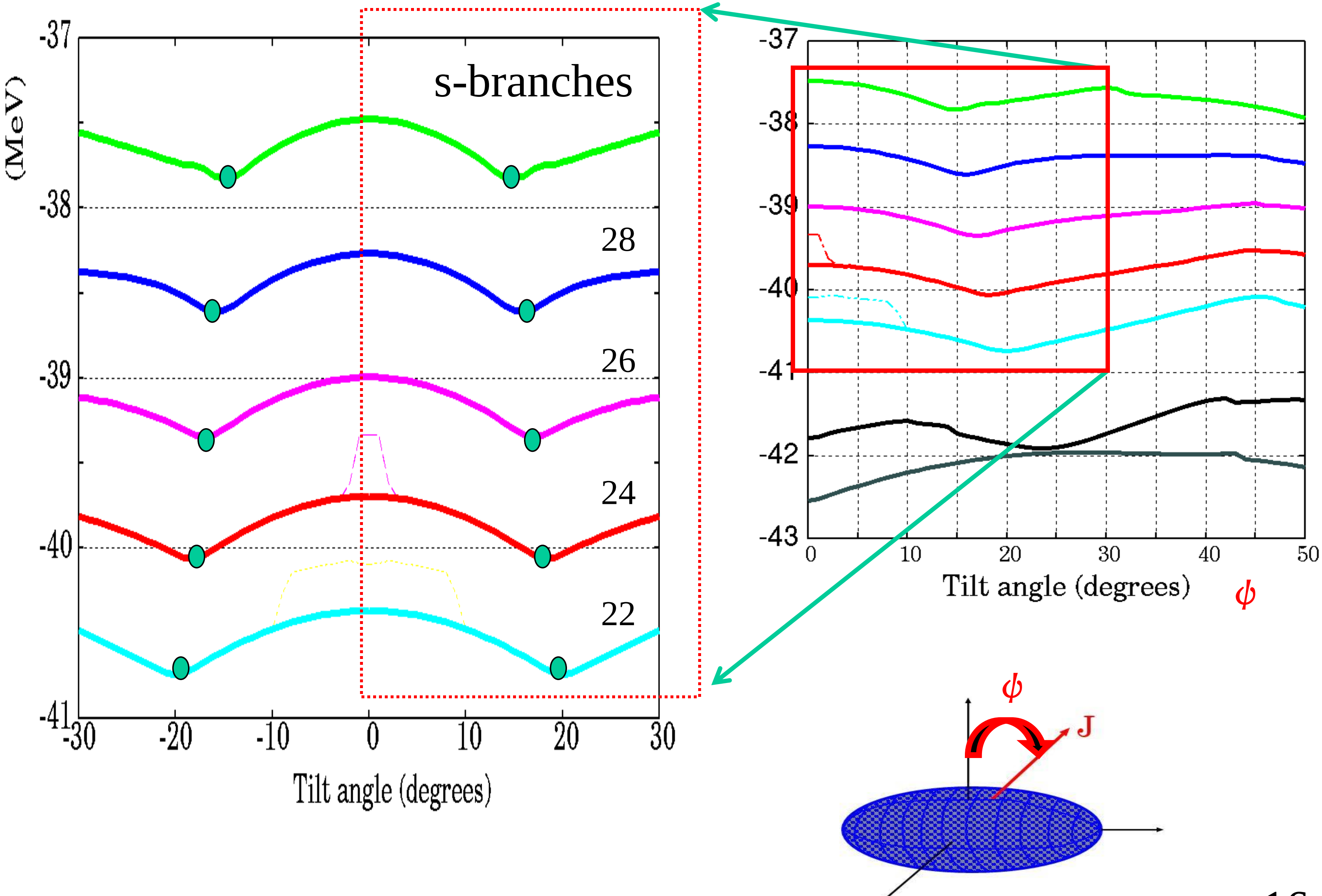

s-branches
(MeV)
-37
-38
-39
-40
-41
28
26
24
22
-30
-20
-10
0
10
20
30
Tilt angle (degrees)
-42
-43
40
50
φ
J

Energy splitting in GCM

generator coordinate a : **tilt angle** ψ

wave function
$$|\Phi\rangle = \int da\ f(a)|\psi(a)\rangle$$

HFB solution at a

$$f(a) \quad \Longleftarrow \quad \delta \frac{\langle\Phi|H|\Phi\rangle}{\langle\Phi|\Phi\rangle} \ = \ 0$$

$$\sum_{k'}\{H_{k,k'} - \lambda_p^{(\alpha)} N^p_{k,k'} - \lambda_n^{(\alpha)} N^n_{k,k'} - \mu^{(\alpha)} \mathbf{J}^2_{k,k'}\} g^{(\alpha)}_{k'} = E^{(\alpha)} g^{(\alpha)}_k$$

Cf. T.Horibata et al., Nucl.Phys.A646(1999), 277.

M.Oi et al., Phys. Lett. B418(1998), 1.

Phys. Lett. B525(2002), 255.

GCM amplitude (－４０ (deg) ～ ＋４０ (deg))

J = 24

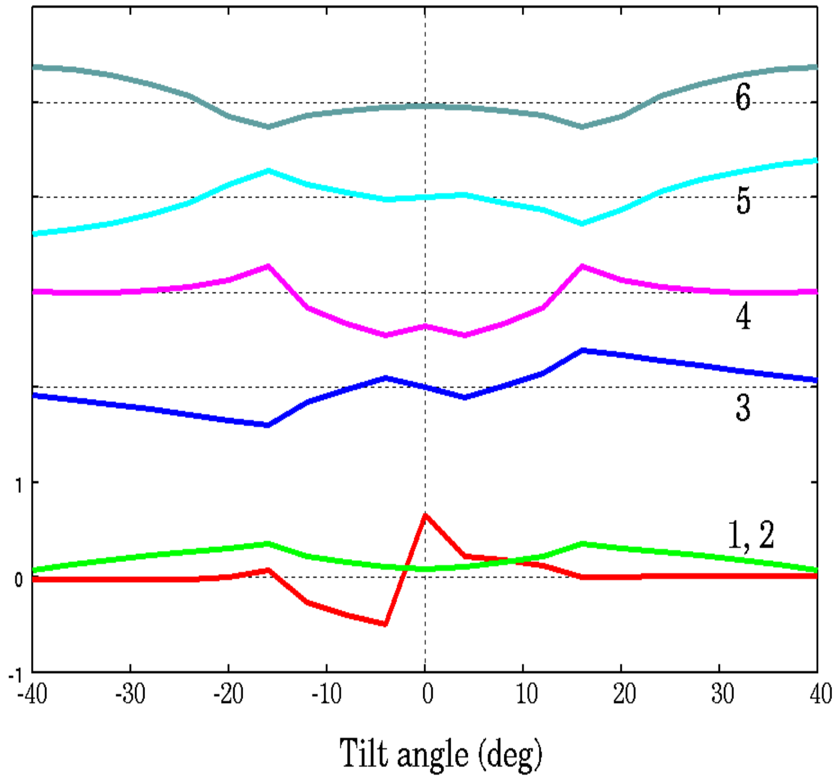

○ Energy splittings

J	ΔE (kev)
２４	１３０
２６	２５２
(２８	９３)

4. Summary

☆ The basic stand point is that the tilted axis band states are realized as a result of the ***tunneling effect***.

○ GCM calculations with J = 24、（２６、２８）were carried out in osmium ^{182}Os

○ Energy splittings are obtained:

J	ΔE (kev)
２４	１３０
２６	２５２
(２８	９３)

○ We need more accurate GCM calculations to explain the experimental data of the tilted axis rotational states.